

Inhibition of CYP1 by 7,8-Dehydrorutaecarpine and Its Methoxylated Derivatives

JEN-CHIH TSENG^{1,2}, MING-JAW DON¹, DAVID F. V. LEWIS³, SHU-YUN WANG¹
AND YUNE-FANG UENG^{1,4*}

¹ National Research Institute of Chinese Medicine, 155-1, Sec. 2, Li-Nong St., Taipei 112, Taiwan (R.O.C.)

² Department of Life Science, Chinese Culture University, Taipei 111, Taiwan (R.O.C.)

³ School of Biomedical and Molecular Sciences, University of Surrey, Guildford GU2 7XH, U.K.

⁴ Graduate Institute of Medical Sciences, Taipei Medical University, Taipei 110, Taiwan (R.O.C.)

ABSTRACT

7,8-Dehydrorutaecarpine was a potent inhibitor of both CYP1A1 and CYP1A2. The introduction of methoxyl group reduced CYP1A1 inhibition and enhanced the relative inhibition selectivity to either CYP1A2 or CYP1B1. Among the synthesized derivatives, 2-methoxy-7,8-dehydrorutaecarpine had the best selectivity of CYP1A2 inhibition. In contrast, the introduction of 4-methoxyl group decreased the IC₅₀ values for CYP1B1 and had the best selectivity of CYP1B1 inhibition. Results of molecular modeling showed that a hydrogen bond was formed between the 2-methoxyl group of 2-methoxy-7,8-dehydrorutaecarpine and Thr¹¹³ residue of CYP1A2. 2-Methoxy-7,8-dehydrorutaecarpine was a mixed type inhibitor of CYP1A2 with the inhibition constants of 9.5 ± 2.6 and 6.7 ± 2.6 nM for CYP1A2 and CYP1A2-substrate complex, respectively. For the 2-methoxyl derivatives of 7,8-dehydrorutaecarpine and rutaecarpine, the change of 2-methoxyl to an 2-ethoxyl group decreased and increased the IC₅₀ values for CYP1A1 and CYP1A2, respectively. Our results demonstrated that introduction of alkoxy modification to a heterocyclic compound, 7,8-dehydrorutaecarpine could change inhibitory selectivity among CYP1 enzymes. These results may provide important information for the interaction between CYP1 members and their inhibitors with a core structure of 7,8-dehydrorutaecarpine.

Key words: CYP1, 7,8-dehydrorutaecarpine, inhibition, selectivity

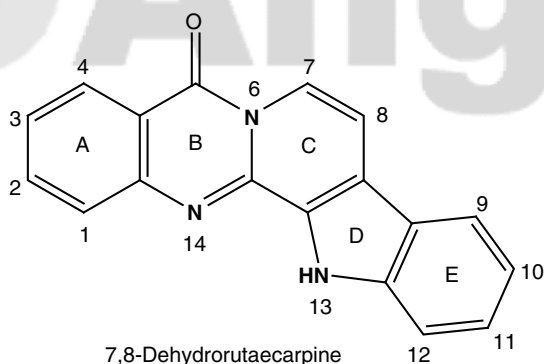
INTRODUCTION

The cytochrome P450 (CYP) 1 family members, CYP1A1, CYP1A2, and CYP1B1 catalyze the crucial steps of detoxification and activation of many endogenous and exogenous compounds including hormones, food-born carcinogens and air pollutants⁽¹⁾. In general, the planar structure is a common characteristic of the CYP1 ligands, such as benzo(a)pyrene, 2-aminoanthracene, estradiol, and α -naphthoflavone⁽²⁾. CYP1 enzymes have overlapped substrate specificity but show differences in regioselectivity and catalytic capacity. CYP1A1 and CYP1A2 have about 80% identity in amino acid sequence and are about 40% identical with CYP1B1⁽¹⁾. Kim *et al.*⁽³⁾ have synthesized a series of alkoxy derivatives of trans-stilbene with enhanced inhibitory effect on CYP1B1. Lewis and Lake⁽⁴⁾ showed that hydrogen bond and π - π stacking interaction are important in the orientation of a ligand in the CYP1A putative active site. It is of interest to assess the orientation

of a ligand affected by the introduction of alkoxy group.

The alkaloid rutaecarpine is a main active constituent of herbal medicine *Evodia rutaecarpa* and has a planar polycyclic structure⁽⁵⁾. Our previous report demonstrated that rutaecarpine is a CYP1A2-selective inhibitor and fitted well in the putative active site of CYP1A2⁽⁶⁾. The IC₅₀ value of rutaecarpine for CYP1A1 was 10-times higher than that of CYP1A2. The introduction of methoxyl substituent(s) enhanced or changed the inhibitory selectivity. Contrary to the CYP1A2-selectivity of rutaecarpine, a synthesized derivative, 7,8-dehydrorutaecarpine (8,13-dihydroindolo[2',3':3,4]pyrido[2,1-b]quinazolin-5-one) (Scheme 1), strongly inhibited CYP1A1 and CYP1A2 with almost equal IC₅₀ values⁽⁶⁾. To clarify the influence of alkoxy modification on CYP1 inhibition, the non-selective inhibitor, 7,8-dehydrorutaecarpine, was studied as a core structure. Its methoxyl and ethoxyl derivatives were synthesized and their IC₅₀ values and inhibitory kinetics were determined. Molecular modeling was employed to understand the interaction of selective inhibitory derivatives with CYP1 members.

* Author for correspondence. Tel: +886-2-2820-1999 ext. 6351;
Fax: +886-2-2826-4266; E-mail: ueng@nricm.edu.tw



Scheme 1. The chemical structure of 7,8-dehydrorutaecarpine.

MATERIALS AND METHODS

I. Chemicals and the Synthesis of Derivatives

7-Ethoxyresorufin, 7-methoxyresorufin, nicotinamide adenine diphosphate (NADP), glucose-6-phosphate, and glucose-6-phosphate dehydrogenase were purchased from Sigma-Aldrich (St. Louis, MO, USA). Trypton, peptone, and yeast extract were purchased from Difco-Becton Dickinson (Sparks, MD, USA). 2,3-dichloro-5,6-dicyano-1,4-benzoquinone (DDQ) was purchased from Merck KGaA (Darmstadt, Germany). 1,4-Dioxane was purchased from Fisher Scientific Inc. (Fair Lawn, New Jersey, USA). Rutaecarpine was synthesized by following the method of Bergman and Bergman⁽⁷⁾. 7,8-Dehydrorutaecarpine was synthesized by dehydrogenation of rutaecarpine with DDQ in dioxane⁽⁷⁾. Methoxyl and ethoxyl derivatives of 7,8-dehydrorutaecarpine were synthesized from the corresponding methoxyl and ethoxyl derivatives of rutaecarpine by treatment with DDQ. The 1-, 2-, 3-, 4-, and 10-methoxyrutaecarpines were prepared as previously described⁽⁶⁾. 2-Ethoxyrutaecarpine was prepared from 1,2,3,4-tetrahydro- β -carboline-1-one⁽⁸⁾ and 2-ethoxyanthranilic acid in the presence of POCl₃⁽⁹⁾. The structures of derivatives were all confirmed with NMR analysis^(7,10).

II. Expression of Human CYP and Enzyme Assays

The plasmids of P450 constructs were kindly provided by Dr. F. Peter Guengerich (Nashville, TN, USA). These constructs were transformed to *Escherichia coli* DH5 α by electroporation (Gene Pulser II, BioRad, Hercules, CA, USA). Bacterial membrane fractions of *E. coli* expressing bicistronic human CYP1A1, CYP1A2, or CYP1B1 were prepared by sonication and differential centrifugation by the method of Parikh *et al.*⁽¹¹⁾. Bacterial membrane fractions were stored at -75°C. Membrane P450 content was determined by the CO-difference spectral method of Omura and Sato⁽¹²⁾. 7-Ethoxyresorufin O-deethylation (EROD) and 7-methoxyresorufin O-demethylation (MROD) activities were determined by

measuring the fluorescence of resorufin⁽¹³⁾. Primarily, 20 pmol P450 and various concentrations (37.5 nM - 2.5 μ M) of 7-ethoxyresorufin or (0.2 - 4.0 μ M) 7-methoxyresorufin were added in 1-mL incubation mixture. The reaction was initiated by a NADPH-generating system containing 0.1 mM NADP, 6 mM glucose-6-phosphate and 0.25 u/ml glucose-6-phosphate dehydrogenase. After incubation at 37°C for 10 min, 2.5 volume of methanol was added to stop reaction. After centrifugation, the fluorescence of supernatant was measured using Hitachi F-4500 fluorescence spectrophotometer (Hitachi Ltd., Tokyo, Japan). The derivatives of 7,8-dehydrorutaecarpine were dissolved in dimethyl sulfoxide (DMSO) and added simultaneously with the substrate 7-ethoxyresorufin in the incubation mixture. The final concentration of DMSO was less than 0.5%.

III. Structural Modeling

Models of human CYP1 family members were generated using the crystal structure of rabbit CYP2C5 as a template based on protein sequence homology following a satisfactory alignment of the relevant sequences⁽²⁾. 7,8-Dehydrorutaecarpine, 2-methoxy-7,8-dehydrorutaecarpine, and 4-methoxy-7,8-dehydrorutaecarpine were respectively fitted within the CYP1A1, CYP1A2, and CYP1B1 putative active sites from the interactive docking. Molecular modeling procedures were carried out using the Sybyl software package (Tripos Associates, St. Louis, MO) implemented on a Silicon Graphics Indigo 10000 graphics workstation operated under UNIX. As the substrate was docked, the formation and breakage of hydrogen bonds between the substrate molecule and active site residues was monitored such that the most energetically (including electrostatic and steric energies) favorable orientation of the substrate was achieved.

IV. Data Analysis

The concentration of a chemical required for 50% inhibition of EROD activity (IC₅₀) was calculated by curve fitting (Grafit, Erithacus Software Ltd., Staines, UK). Values of velocities (v) at various substrate concentrations (S) were fitted by nonlinear least-squares regression without weight due to the equation, consistent with the following inhibition types according to the Michaelis-Menten equation: (1) competitive inhibition: $v = V_{max} \cdot S / (K_m [1 + (I/K_i)] + S)$; (2) noncompetitive inhibition: $v = V_{max} \cdot S / (K_m + S) [1 + (I/K_i)]$; (3) mixed type: $v = V_{max} \cdot S / (K_m [1 + (I/K_i)] + S [1 + (I/K_I)])$. The V_{max} and I are the maximal velocity and inhibitor concentration, respectively (Sigma Plot, Jandel Scientific, San Rafael, CA, USA). The inhibition constants, K_i and K_I are the constants for P450 and P450-substrate complex, respectively. For noncompetitive inhibition, K_i is equal to K_I . Estimates of variance (internal estimates of error, denoted by \pm) are presented from analyses of individual sets of data.

Table 1. Kinetic analysis of O-dealkylations of 7-ethoxyresorufin and 7-methoxyresorufin catalyzed by *E. coli* membrane-expressing human CYP1A1, CYP1A2, and CYP1B1

Enzymes	K_m , μM	V_{max} , nmol/min/nmol P450	Clint (V_{max}/K_m), mL/min/nmol P450
7-Ethoxyresorufin O-deethylation			
CYP1A1	1.80 \pm 0.67	59.4 \pm 10.2	33
CYP1A2	0.82 \pm 0.17	10.9 \pm 0.9	12
CYP1B1	0.39 \pm 0.05	11.7 \pm 0.8	30
7-Methoxyresorufin O-demethylation			
CYP1A1	1.80 \pm 0.33	18.1 \pm 1.6	10
CYP1A2	2.67 \pm 0.41	20.6 \pm 1.7	8
CYP1B1	0.35 \pm 0.14	1.3 \pm 0.2	4

Kinetic parameters were determined using the nonlinear regression without weight as described in the Materials and Methods. Determination was performed with duplicates. Estimates of variance (denoted by \pm) are presented from analysis of individual sets of data.

RESULTS AND DISCUSSION

7-Ethoxyresorufin is a common substrate of CYP1 members. In the study of mouse P450 induction, comparison of the inducibility by 2,3,7,8-tetrachlorodibenzo-*p*-dioxin (TCDD) and 3-methylcholanthrene suggested that CYP1A1 and CYP1A2 showed respective preference for the O-dealkylations of 7-ethoxyresorufin and 7-methoxyresorufin⁽¹⁴⁾. For EROD, our results showed that CYP1A1 had the highest V_{max} (59.4 nmol/min/nmol P450) and intrinsic clearance (33 mL/min/nmol P450) values (Table 1). However, the K_m values were in the order of CYP1B1 < CYP1A2 < CYP1A1. CYP1A1 did not have the lowest K_m value, suggesting that its high catalytic activity was not attributed to high binding affinity. In consistent with our results, Shimada *et al.*⁽¹⁵⁾ also reported that CYP1A1 had the highest intrinsic clearance but with a relatively high K_m value in the study of yeast microsomes expressing CYP1B1 and *E. coli* membrane expressing CYP1A1 or CYP1A2. However, Chaudhary and Willett⁽¹⁶⁾ reported that K_m values for CYP1A1 and CYP1B1 were 0.054 and 0.35 μM , respectively. The K_m value for CYP1B1 was similar to our determination. In contrast, the K_m value for CYP1A1 was much less than our determination. The P450 concentration was not determined in this report. Difference in P450 concentration in the assay can result in different K_m value. For MROD, the K_m and V_{max} values of CYP1A1 and CYP1A2 were similar. However, CYP1B1 had K_m and V_{max} values less than 20% of the respective values of CYP1A1 and CYP1A2. CYP1A1 had an intrinsic clearance of MROD about 30% of EROD. Molecular dynamic simulation analysis suggested that 7-ethoxyresorufin and 7-methoxyresorufin bound to CYP1A1 without major steric hinderance⁽¹⁷⁾. In consistent with this report, our results showed that CYP1A1 had same K_m values for EROD and MROD. Szklarz and Paulsen⁽¹⁸⁾ reported that the distance between the ferryl oxygen in the active site of CYP1A1 and hydrogens of 7-ethoxyresorufin at the oxidation site was less than the distance for 7-methoxyresoru-

Table 2. The inhibition of 7-ethoxyresorufin O-deethylation activities of human CYP1A1, CYP1A2, and CYP1B1 by dehydrorutaecarpine derivatives

Parent compounds and their derivatives	IC ₅₀ , nM		
	CYP1A1	CYP1A2	CYP1B1
7,8-Dehydrorutaecarpine ^a	32 \pm 3	30 \pm 4	69 \pm 22
1-Methoxy-	501 \pm 28	30 \pm 7	32 \pm 2
2-Methoxy-	266 \pm 35	10 \pm 1	60 \pm 2
2-Ethoxy-	138 \pm 5	58 \pm 6	260 \pm 6
3-Methoxy-	1408 \pm 56	36 \pm 3	69 \pm 5
4-Methoxy-	1605 \pm 49	77 \pm 20	8.2 \pm 0.3
10-Methoxy-	644 \pm 26	86 \pm 3	171 \pm 3
Rutaecarpine ^a	260 \pm 30	22 \pm 3	55 \pm 11
1-Methoxy- ^a	450 \pm 90	11 \pm 0	71 \pm 10
2-Methoxy- ^a	850 \pm 50	76 \pm 8	170 \pm 8
10-Methoxy- ^a	1780 \pm 380	2920 \pm 690	84 \pm 17
2-Ethoxy-	624 \pm 33	159 \pm 12	249 \pm 8

Concentrations of 7-ethoxyresorufin and P450 were 2 μM and 20 nM in the assay, respectively. Rutaecarpine, dehydrorutaecarpine, and their derivatives were dissolved in DMSO. The same volume of DMSO was added to the control and the final concentration of DMSO was less than 0.5%. Determination was performed with duplicates. Estimates of variance (denoted by \pm) are presented from the analysis of individual sets of data. ^aData were reported in previous report (Don *et al.*, 2003).

fin binding. The non-bond enzyme-substrate interaction energy of CYP1A1 for 7-ethoxyresorufin was lower than that for 7-methoxyresorufin. This may explain the high intrinsic clearance of 7-ethoxyresorufin by CYP1A1.

For 7,8-dehydrorutaecarpine, the introduction of a methoxyl group at C2, C3, and C10 enhanced inhibition selectivity of CYP1A2 with IC₅₀ ratios \geq 2 for both CYP1A1/CYP1A2 and CYP1B1/CYP1A2 (Table 2). The introduction of these methoxyl groups highly

increased the IC_{50} values for CYP1A1 by 4- to 50-fold as compared with the lead compound, 7,8-dehydrorutaecarpine. The increase in IC_{50} values for CYP1A1 is one factor for increase CYP1A2 selectivity by these methoxyl derivatives. Besides of the reduction of CYP1A1 inhibition potency, the introduction of 2-methoxyl moiety also enhanced CYP1A2 inhibition by reducing the IC_{50} value (Table 2). In contrast, the introduction of a methoxyl group at C4 caused a CYP1B1-selective inhibition. Among the derivatives studied, the most potent and selective CYP1A2 inhibitor was 2-methoxy-7,8-dehydrorutaecarpine with the IC_{50} ratios of 27 and 6 for CYP1A1/CYP1A2 and CYP1B1/CYP1A2, respectively. The elongation of the 2-methoxyl moiety to an ethoxyl group caused a 50% decrease and a 6-fold increase of the IC_{50} values for CYP1A1 and CYP1A2, respectively (Table 2). In consistent with these changes, the change of 2-methoxyl modification of rutaecarpine to an ethoxyl group also decreased and increased the IC_{50} values for CYP1A1 and CYP1A2, respectively. The actual cause of this phenomenon is not known. According to the lower CYP1A1 interaction energy for 7-ethoxyresorufin than 7-methoxyresorufin⁽¹⁸⁾, one possible cause would be the differences in the binding energy of methoxyl and ethox-

yl derivatives to CYP1A1/CYP1A2 and this needs further studies. It is of interest to investigate the effects of other alkoxyl derivatives, such as propanoxyl and butanoxyl derivatives in the future.

For comparison of the respective CYP1A2 and CYP1B1 selectivity of 2-methoxy-7,8-dehydrorutaecarpine and 4-methoxy-7,8-dehydrorutaecarpine, structural modeling was analyzed. Similar to our previous report of the CYP1A2-binding of rutaecarpine⁽⁶⁾, hydrogen bond and the π - π stacking are still important factors of 7,8-dehydrorutaecarpine and its derivatives (Figure 1). One hydrogen bond can be formed between the keto-group of 7,8-dehydrorutaecarpine and Ser¹¹³ residue of CYP1A1 (Figure 1A). The A- and D-rings of 7,8-dehydrorutaecarpine formed π - π stacking interactions with the aromatic ring of Phe³⁵⁸ and Phe²⁰⁵ residues of CYP1A1, respectively. However, our previous study of the structural modeling shows that the best fit allows the E-ring moiety of rutaecarpine to approach the heme moiety of CYP1A2 active site pocket⁽⁶⁾. In this report, our results showed that the best fitting allowed the A-ring of 7,8-dehydrorutaecarpine to approach the heme moiety of CYP1A1. Although the amino acid sequence identity of CYP1A1 and CYP1A2 is higher than 80%, several amide resi-

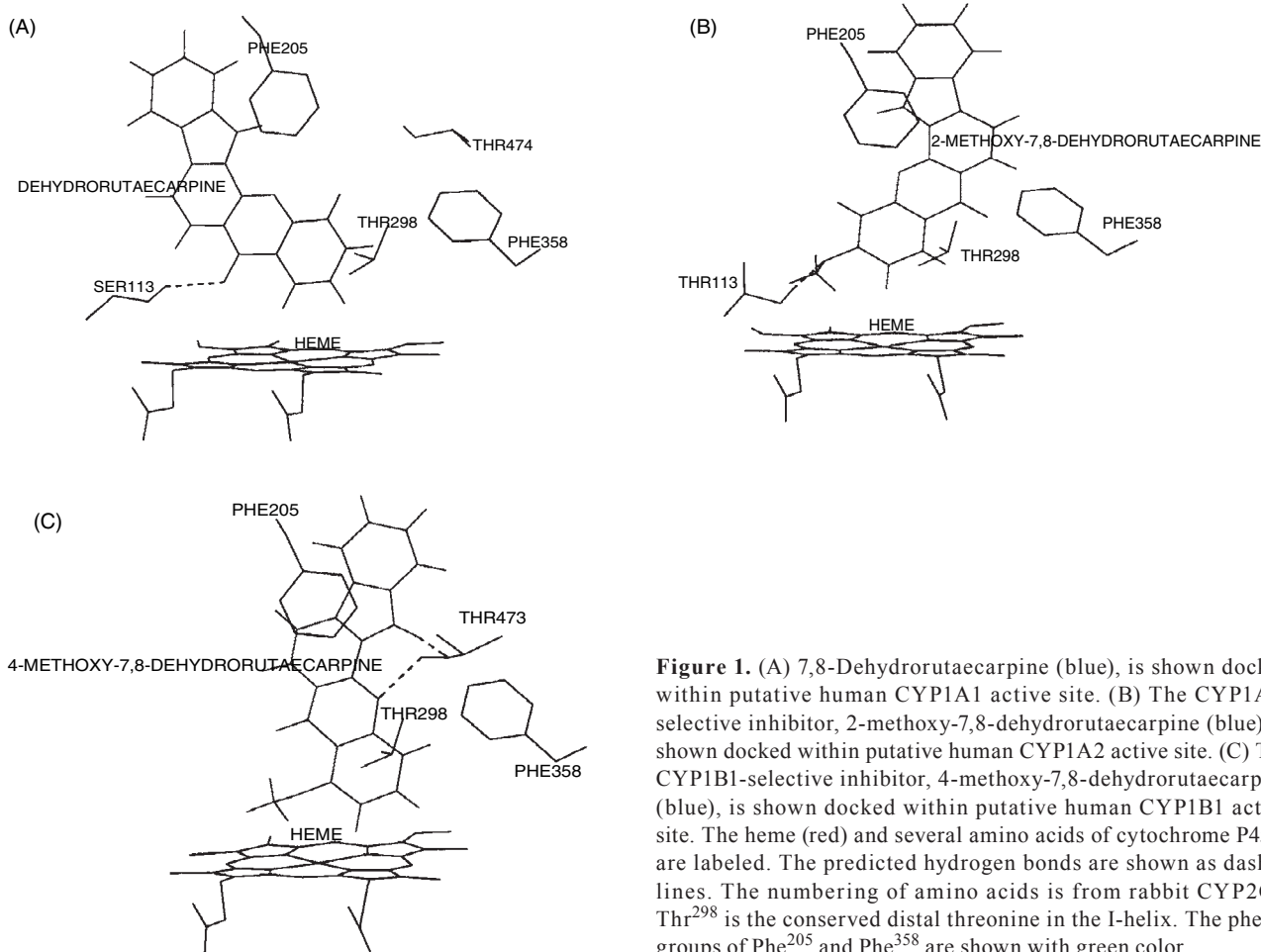


Figure 1. (A) 7,8-Dehydrorutaecarpine (blue), is shown docked within putative human CYP1A1 active site. (B) The CYP1A2-selective inhibitor, 2-methoxy-7,8-dehydrorutaecarpine (blue), is shown docked within putative human CYP1A2 active site. (C) The CYP1B1-selective inhibitor, 4-methoxy-7,8-dehydrorutaecarpine (blue), is shown docked within putative human CYP1B1 active site. The heme (red) and several amino acids of cytochrome P450s are labeled. The predicted hydrogen bonds are shown as dashed lines. The numbering of amino acids is from rabbit CYP2C5. Thr²⁹⁸ is the conserved distal threonine in the I-helix. The phenyl groups of Phe²⁰⁵ and Phe³⁵⁸ are shown with green color.

dues around the CYP1A2 substrate binding site become aromatic or hydrophobic residues in CYP1A1⁽⁴⁾. This may cause the differential orientation of 7,8-dehydrorutaecarpine in CYP1A1 active site.

The best fitting allowed the A-ring of the CYP1A2-selective inhibitor, 2-methoxy-7,8-dehydrorutaecarpine to approach the heme moiety of CYP1A2 (Figure 1B). A hydrogen bond was formed between the 2-methoxyl moiety and Thr¹¹³ residue of CYP1A2. This may contribute to the low IC₅₀ value of 2-methoxy-7,8-dehydrorutaecarpine for CYP1A2 (Table 2). The active sites of CYP1B1 and CYP1A2 have several differences including the hydrogen bond donor/acceptor of the side chains^(4,19). These differences may be associated with differential inhibitory selectivity of methoxyl derivatives. Our results showed that CYP1B1 selective inhibitor, 4-methoxy-7,8-dehydrorutaecarpine fitted well with the putative active sites of CYP1B1 (Figure 1C). The A-ring of 4-methoxy-7,8-dehydrorutaecarpine approached the heme moiety of CYP1B1. Different from the binding to CYP1A2, the core structure flipped in another side and allowed the formation of two hydrogen bonds at N13 and N14 with amino acid residues. This result indicated the good fitting of 4-methoxy-7,8-dehydrorutaecarpine to CYP1B1 active site.

Results of inhibitory kinetic analysis showed that 7,8-dehydrorutaecarpine and its CYP1A2-selective derivative, 2-methoxy-7,8-dehydrorutaecarpine caused a mixed type inhibition of CYP1A2 with the inhibition constants of 9.5 ± 2.6 and 6.7 ± 2.6 nM for CYP1A2 and CYP1A2-substrate complex, respectively (Figure 2 and Table 3). These results revealed that 7,8-dehydrorutaecarpine and 2-methoxy-7,8-dehydrorutaecarpine are bound to both CYP1A2 and CYP1A2-substrate complex. For comparison, the inhibitory kinetic parameters of rutaecarpine and its derivatives were determined. Like 7,8-dehydrorutaecarpine, rutaecarpine was a mixed type inhibitor of CYP1A2. The highly CYP1A2-selective derivative of rutaecarpine, 1-methoxyrutaecarpine caused a competitive inhibition, suggesting a binding to CYP1A2. For CYP1B1 inhibition, 7,8-dehydrorutaecarpine caused a mixed type inhibition of CYP1B1 (Figure 3 and Table 4). The CYP1B1-selective derivative, 4-methoxy-7,8-dehydrorutaecarpine also caused mixed type inhibition of CYP1B1. However, rutaecarpine was a noncompetitive inhibitor of CYP1B1. The CYP1B1-selective derivative, 10-methoxyrutaecarpine caused a mixed type inhibition. These results revealed that 7,8-dehydrorutaecarpine, 4-methoxy-7,8-dehydrorutaecarpine, rutaecarpine, and 10-methoxyrutaecarpine are bound to both CYP1B1 and CYP1B1-substrate complex.

In summary, our results demonstrated that the introduction of a methoxyl group to C2, C3, and C10 of 7,8-dehydrorutaecarpine shifted the CYP1 inhibition from non-selective to CYP1A2-selective inhibition. 2-Methoxy-7,8-dehydrorutaecarpine showed the best inhibitory selectivity of CYP1A2 with mixed type inhi-

Table 3. The inhibitory parameters of derivatives on 7-ethoxyresorufin *O*-deethylation activity of human CYP1A2

Compound	Type	Inhibition constant
7,8-Dehydrorutaecarpine	Mixed	K _i = 10.3 ± 1.2 nM
		K _i = 5.3 ± 0.3 nM
2-Methoxy-7,8-dehydrorutaecarpine	Mixed	K _i = 9.5 ± 2.6 nM
		K _i = 6.7 ± 2.6 nM
Rutaecarpine	Mixed	K _i = 109 ± 52 nM
		K _i = 27 ± 4 nM
1-Methoxyrutaecarpine	Competitive	K _i = 6.3 ± 0.8 nM

For inhibition kinetics determination, increasing concentrations of 7-ethoxyresorufin were used in the assay (Figure 2). The type of inhibition was analyzed by Lineweaver-Burk plot. Inhibition constants were calculated by non-linear regression as described in Materials and methods. Determination was performed with duplicates. Estimates of variance (denoted by ±) are presented from the analysis of individual sets of data.

Table 4. The kinetic parameters of derivatives on 7-ethoxyresorufin *O*-deethylation activity of human CYP1B1

Compound	Type	Inhibition constant
7,8-Dehydrorutaecarpine	Mixed	K _i = 245 ± 82 nM
		K _i = 35 ± 3 nM
4-Methoxy-7,8-dehydrorutaecarpine	Mixed	K _i = 19 ± 2 nM
		K _i = 12 ± 1 nM
Rutaecarpine	Noncompetitive	K _i = 60 ± 10 nM
10-Methoxyrutaecarpine	Mixed	K _i = 231 ± 30 nM
		K _i = 95 ± 8 nM

For inhibition kinetics determination, increasing concentrations of 7-ethoxyresorufin were used in the assay (Figure 4). Inhibition constants were calculated by non-linear regression as described in Materials and methods. Determination was performed with duplicates. Estimates of variance (denoted by ±) are presented from the analysis of individual sets of data.

bition. For both 7,8-dehydrorutaecarpine and rutaecarpine, the change of 2-methoxyl to 2-ethoxyl modification decreased and increased the IC₅₀ values for CYP1A1 and CYP1A2, respectively. CYP1 enzymes play differential roles in the activation of different groups of carcinogens. Chemical inhibitors are commonly used for the identification of P450 forms involved in xenobiotic oxidation. Our results provide important information for the interaction between CYP1 members and inhibitors with a core structure of 7,8-dehydrorutaecarpine.

ACKNOWLEDGEMENTS

This work was supported by National Research Institute of Chinese Medicine and NSC 95-2320-B-077-005-MY2 from National Science Council, Taipei, Taiwan.

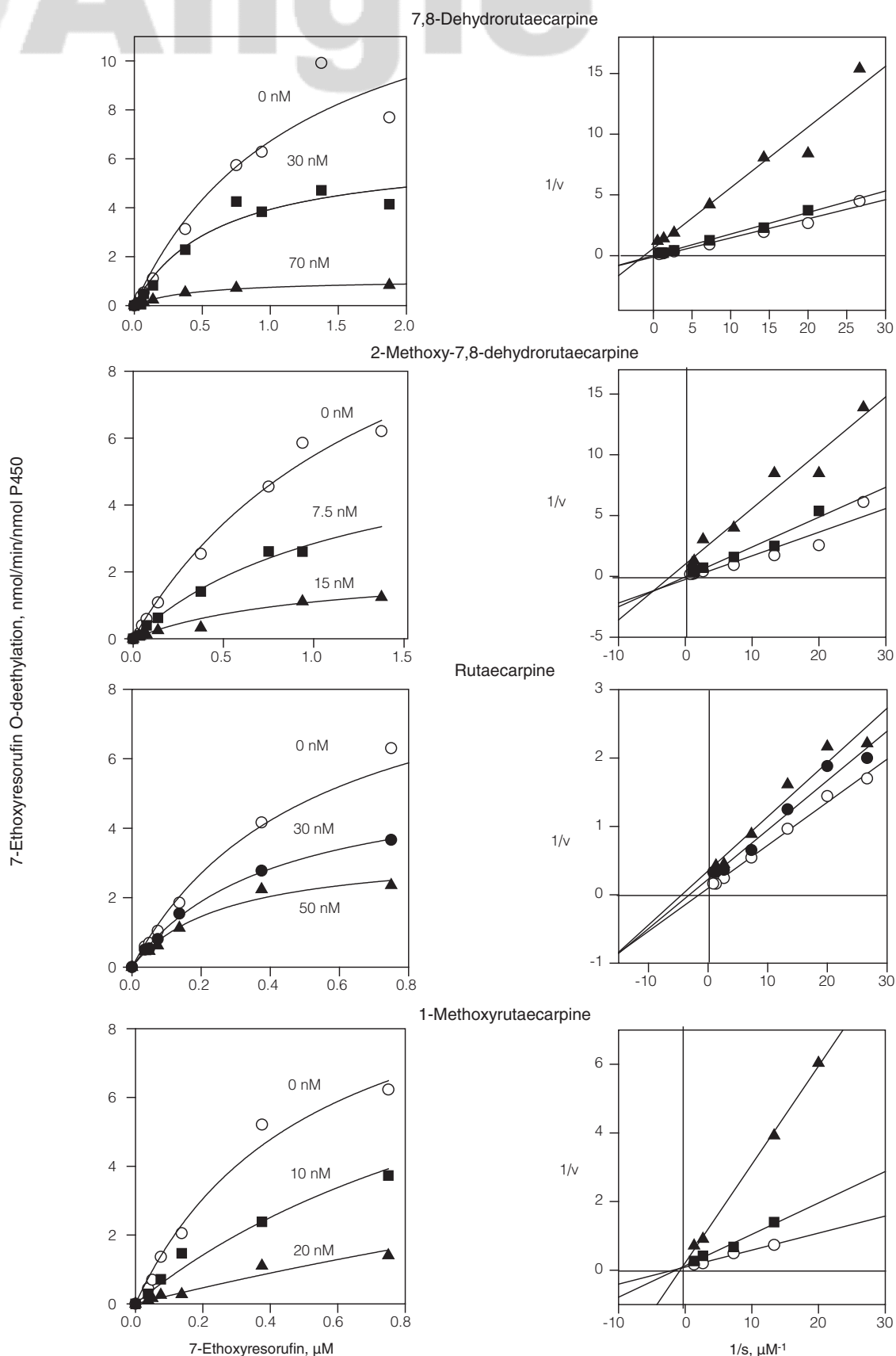


Figure 2. Inhibition kinetic analysis of methoxyl derivatives of dehydrorutaecarpine and rutaecarpine on CYP1A2-catalyzed 7-ethoxyresorufin O-deethylation activity. Determination was performed with duplicates. Right panel: the velocity (v) versus substrate concentration (s) plots. Left panel: the Lineweaver-Burk plot. Solid lines represent the lines of best fit as determined by nonlinear or linear regressions as described in the section of Materials and Methods. The concentrations of inhibitors are shown in the figures.

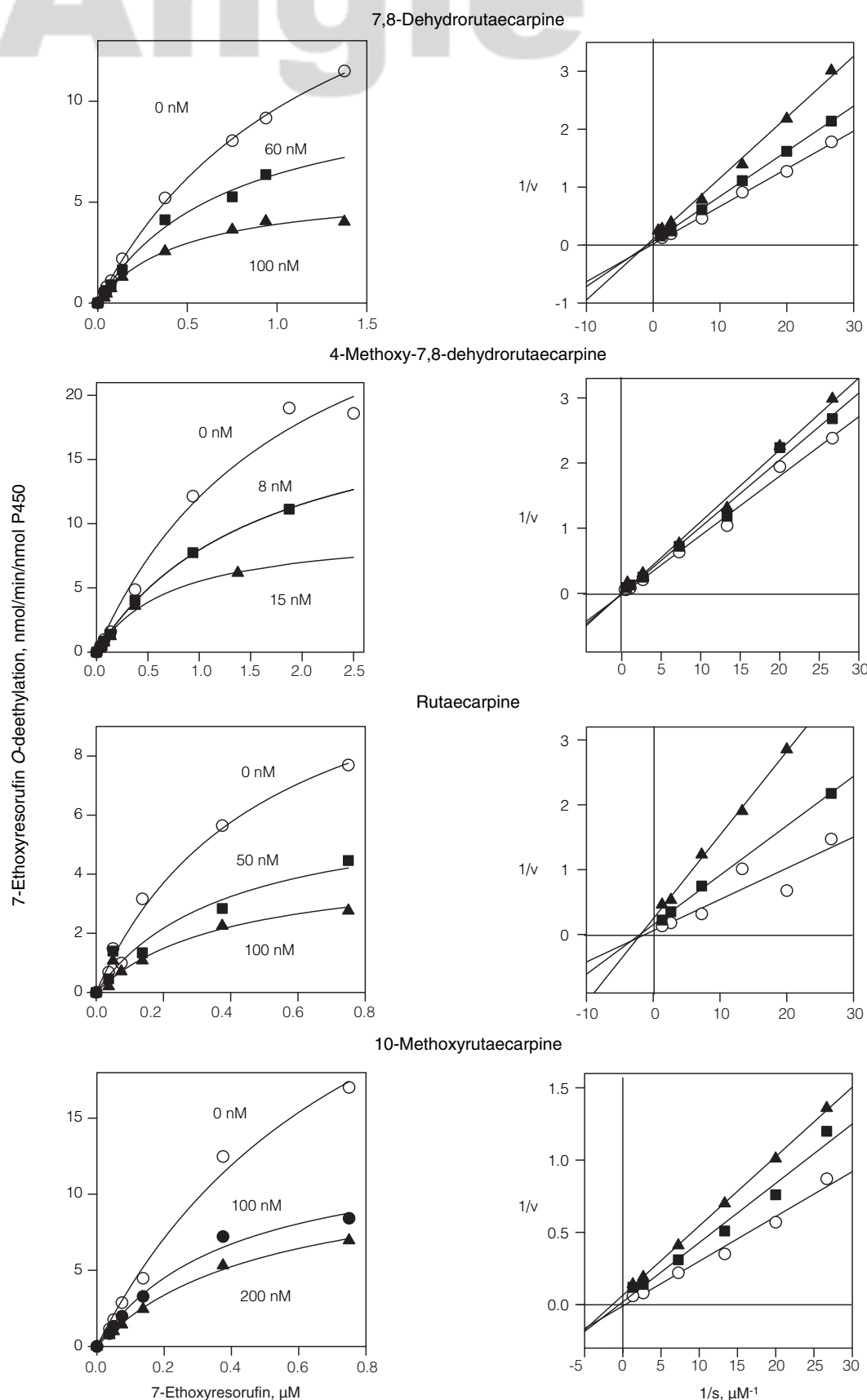


Figure 3. Inhibition kinetic analysis of methoxyl derivatives of dehydrorutaecarpine and rutaecarpine on CYP1B1-catalyzed 7-ethoxyresorufin *O*-deethylation activity. Determination was performed with duplicates. Right panel: the velocity (v) versus substrate concentration (s) plots. Left panel: the Lineweaver-Burk plot. Solid lines represent the lines of best fit as determined by nonlinear or linear regressions as described in the section of Materials and Methods. The concentrations of inhibitors are shown in the figures

REFERENCES

1. Guengerich, F. P. 1995. Human cytochrome P450. In "Cytochrome P450". pp 473-535. Ortiz de Montelano, P. R. ed. Plenum Press, New York.
2. Lewis, D. F. V., Lake, B. G., Dickins, M., Ueng, Y. F. and Goldfarb, P. S. 2003. Homology modeling of human CYP1A2 based on the CYP2C5 crystallographic template structure. *Xenobiotica* 33: 239-254.
3. Kim, S., Ko, H., Park, J. E., Jung, S., Lee, S. K., and Chun, Y. J. 2002. Design, synthesis, and discovery of novel trans-stilbene analogues as potent and selective human cytochrome P450 1B1 inhibitors. *J. Med. Chem.* 45: 160-164.
4. Lewis, D. F. V. and Lake, B. G. 1996. Molecular modeling of CYP1A subfamily members based on an alignment with CYP102: rationalization of CYP1A substrate specificity in terms of active site amino acid residues. *Xenobiotica* 16: 723-753.
5. Sheu, J. R. 1999. Pharmacological effects of rutaecarpine, an alkaloid isolated from *Evodia rutaecarpa*. *Cardiovasc. Drug Rev.* 17: 237-245.
6. Don, M. J., Lewis, D. F. V., Wang, S. Y., Tsai, M. W. and Ueng, Y. F. 2003. Effect of structural modification on the inhibitory selectivity of rutaecarpine derivatives on human CYP1A1, CYP1A2, and CYP1B1. *Bioorg. Med. Chem. Lett.* 13: 2535-2538.
7. Bergman, J. and Bergman, S. 1985. Studies of rutaecarpine and related quinazolinocarboline alkaloids. *J. Organic Chem.* 50: 1246-1255.
8. Narayanan, K., Schindler, L. and Cook, J. M. 1991. Carboxyl-Mediated Pictet-Spengler Reaction. Direct Synthesis of 1,2,3,4-Tetrahydro- β -carbolines from Tryptamine-2-carboxylic Acids. *J. Organ. Chem.* 56: 359-365.
9. Danieli, B., Palmisano, G., Rainoldi, G. and Russo, G. 1974. 1-Hydroxyrutaecarpine from *Euxylophora Paraënsis*. *Phytochemistry* 13: 1603-1606.
10. Yang, L. M., Chen, C. F. and Lee, K. H. 1995. Synthesis of rutaecarpine and cytotoxic analogues. *Bioorg. Med. Chem. Lett.* 5: 465-468.
11. Parikh, A., Gillam, E. M. J. and Guengerich, F. P. 1997. Drug metabolism by *Escherichia coli* expressing human cytochrome P450. *Natur. Biotech.* 15: 784-788.
12. Omura, T. and Sato, R. 1964. The carbon monoxide-binding pigment of liver microsomes. I. Evidence for its heme protein nature. *J. Biol. Chem.* 239: 2370-2379.
13. Pohl, R. J. and Fouts, J. R. 1980. A rapid method for assaying the metabolism of 7-ethoxyresorufin by microsomal subcellular fractions. *Anal. Biochem.* 107: 150-155.
14. Gradelet, S., Astrog, P., Pineau, T., Canivenc, M. C., Siess, M. H., Leclerc, J. and Lesca, P. 1997. Ah receptor-dependent CYP1A induction by two carotenoids, canthaxanthin and β -apo-8'-carotenal with no affinity for the TCDD binding site. *Biochem. Pharmacol.* 54: 307-315.
15. Shimada, T., Gillam, E. M. J. Sutter, T. R., Strickland, P. T., Guengerich, F. P. and Yamazaki, H. 1997. Oxidation of Xenobiotics by Recombinant Human Cytochrome P450 1B1. *Drug Metab. Dispos.* 25: 617-622.
16. Chaudhary, A. and Willett, K. L. 2006. Inhibition of human cytochrome CYP1 enzymes by flavonoids of St. John's wort. *Toxicol.* 217: 194-205.
17. Liu, J., Ericksen, S. S., Besspiata, D., Fisher, C. W. and Szklarz, G. D. 2003. Characterization of substrate binding to cytochrome P450 1A1 using molecular modeling and kinetic analyses: case of residue 382. *Drug Metab. Dispos.* 31: 412-420.
18. Szklarz, G. D. and Paulsen, M. D. 2002. Molecular modeling of cytochrome P4501A1: enzyme-substrate interactions and substrate binding affinities. *J. Biomol. Struc. Dynam.* 20: 155-162.
19. Lewis, D. F. V., Lake, B. G., George, S. G., Dickins, M., Eddershaw, P. J., Tarbit, M. H., Bereford, A. P., Goldfarb, P. S. and Guengerich, F. P. 1999. Molecular modelling of CYP1 family enzymes CYP1A1, CYP1A2, CYP1A6 and CYP1B1 based on sequence homology with CYP102. *Toxicology* 139: 53-79.